Accepted Manuscript

Title: Electrocoagulation of raw wastewater using aluminum, iron, and magnesium electrodes

Authors: Tanner Ryan Devlin, Maciej S. Kowalski, Efren Pagaduan, Xugang Zhang, Victor Wei, Jan A. Oleszkiewicz

PII: S0304-3894(18)30917-8
DOI: https://doi.org/10.1016/j.jhazmat.2018.10.017
Reference: HAZMAT 19837

To appear in: *Journal of Hazardous Materials*

Received date: 27-9-2017
Revised date: 5-10-2018
Accepted date: 8-10-2018

Please cite this article as: Ryan Devlin T, Kowalski MS, Pagaduan E, Zhang X, Wei V, Oleszkiewicz JA, Electrocoagulation of raw wastewater using aluminum, iron, and magnesium electrodes, *Journal of Hazardous Materials* (2018), https://doi.org/10.1016/j.jhazmat.2018.10.017

Electrocoagulation of raw wastewater using aluminum, iron, and magnesium electrodes

Tanner Ryan Devlin, Maciej S. Kowalski, Efren Pagaduan, Xugang Zhang, Victor Wei, Jan A. Oleszkiewicz

Department of Civil Engineering, University of Manitoba, Winnipeg, Canada, R3T 5V6

* Email: umdevli5@myumanitoba.ca

Highlights

- Max. COD removal at 600 mA for 30 min:Al-Al=68±9%; (Fe-Fe)+air=60±30%; and Mg-Mg=27±3%.
- Max. OP removal rates (i.e., mg-P/mmol-e):Al-Al, Fe-Fe, and (Fe-Fe)+air=6.8; Mg-Mg=0.9.
- <0.5 mg-P/L OP achieved in all cases at linearized rate.
- Electrocoagulation did not consume alkalinity.
- Electrocoagulation with aluminum improved nitrification rates.

ABSTRACT

Primary influent from a municipal wastewater treatment plant was electrochemically treated with sacrificial aluminum, iron, and magnesium electrodes. The influence of sacrificial

anodes on the removal of chemical oxygen demand, total nitrogen, total phosphorus, and orthophosphate during sedimentation was investigated. Nitrification kinetics were assessed on treated supernatant and biogas production was monitored on settled solids. Changes in alkalinity, conductivity, and pH were also recorded. Aluminum and iron electrodes provided high rates of orthophosphate removal (i.e., 6.8 mg-P/mmol-e). Aluminum and iron electrodes also provided similar treatment to equivalent doses of alum and ferric salts (i.e., 38-68% chemical oxygen demand, 10-13% total nitrogen, and 67-93% total phosphorus). The estimated stochiometric ratio of aluminum and iron dosed to orthophosphate removed was approximately 1.3:1 and 4.1:1, respectively. Magnesium electrodes, on the other hand, removed orthophosphate at rates 8-9 times slower than aluminum and iron (i.e., 0.9 mg-P/mmol-e). Magnesium had to be dosed at a ratio of 13.5:1 orthophosphate for phosphorus removal. Orthophosphate removal by magnesium electrodes was most likely limited by electrolysis reactions responsible for increases in pH (i.e., 0.52 pH units/ mmol-e). Magnesium electrodes removed 49% chemical oxygen demand and 21% total nitrogen at the high molar ratios required for orthophosphate removal.

Keywords

Municipal wastewater, Electrocoagulation, Phosphorus, Nitrification, Anaerobic digestion

1. Introduction

Wastewater treatment plants (WWTP) receive complex mixtures of nutrients and organic/inorganic pollutants from both municipal and industrial sources. Economies of scale allow for large urban centres to apply advanced treatment technologies with less of a burden on residents [1]. Therefore, most large WWTPs are adequately designed to remove the

pollutant load from wastewaters before they enter the environment. In contrast, smaller communities, especially in locations such as Canada's North or remote Australian communities, do not benefit from the same economies of scale [2,3]. Compounding factors such as inadequate or non-existent transportation infrastructure and lack of highly qualified personnel drives the cost of WWTPs up in small communities. Deficiencies in WWTPs and sanitation in general create exposure pathways by which transmissible enteric, skin, eye, and other disease can be contracted and subsequently spread among the community [4]. This has resulted in millions of preventable deaths each year among populations at risk [5]. Thus, wastewater as well as WWTP discharge in small communities may be considered a hazardous material capable of inflicting harm through unintentional direct contact, cross contamination of drinking water sources, or bioaccumulation of contaminants such as metals in the food chain [6,7].

Successful treatment of wastewater in small, remote communities requires the development of reliable processes that minimize external requirements (i.e., chemicals and electricity) and have a high degree of robustness to address daily, seasonal, and irregular changes in wastewater characteristics. In general, wastewater can be treated biologically, chemically, or with a combination of both [8–10]. Chemical treatments tend to be reliable but require regular shipments of metal salts or other chemical mixtures. Especially for remote communities, the shipment of conventional chemicals such as alum and ferric may be an expensive and unreliable endeavour. The ideal chemical process for wastewater treatment in remote communities would operate with low consumables while significantly improving the capacity of downstream mechanical plants, lagoons, or passive treatment systems such as

wetlands by diverting more of the organic load to stabilization processes such as composting or digestion [11,12]. Diversion of particulate organics could also improve nitrification since less oxygen would be required for the oxidation of organic material [13]. Furthermore, diversion of particulate organics could enhance stabilization processes due to higher biodegradability of the diverted stream compared to biomass that would have been generated if the particulate organics were not diverted [14].

Electrocoagulation processes generate coagulants in situ through electrolytic oxidation. The coagulant, typically generated by aluminum or iron sacrificial anodes, removes colloidal matter while entrapping additional compounds such as orthophosphates [15]. The advantages of electrocoagulation include simple and easily operated equipment, reliable and effective treatment, as well as the formation of flocs that settle well and are easily dewatered [16]. Previous studies have demonstrated chemical oxygen demand (COD) removal of up to 75% during primary treatment [17]. It has also been demonstrated to be an energy efficient option to achieve low orthophosphate residuals, with iron electrodes providing the lowest cost [18]. Electrocoagulation processes should therefore be of interest to remote communities for their low power requirements, capabilities to enhance primary sedimentation, use of dense material that is more convenient to transport, and minimal impact on water chemistry such as alkalinity and pH that will not affect downstream processes such as nitrification [19]. Furthermore, novel electrode materials such as magnesium may provide for nutrient recovery, as magnesium-phosphate complex (e.g., struvite), in addition to improved operations such as stabilization [20].

In this study, primary influent (PI) from a WWTP in Winnipeg, Canada was subjected to electrocoagulation with aluminum (Al-Al), iron (Fe-Fe), and magnesium (Mg-Mg) electrodes in 10 L batch tests. Removal efficiencies for organics and nutrients were measured and compared to a control (i.e., sedimentation). Furthermore, nitrification kinetics were quantified in the treated supernatants and anaerobic stabilization of settled solids was analyzed by volatile solids destruction and biogas potential. The objective was to elucidate design parameters for electrocoagulation processes while studying magnesium electrodes as a novel sacrificial anode material with potential for mainstream phosphorus recovery.

2. Material and methods

2.1. Reactor, electrochemical device, and wastewater characteristics

An acrylic continuously stirred-tank reactor (CSTR) with a working volume of 10 L was used for experimentation. The CSTR was mixed with a magnetic mixer and stirring bar at approximately 120 rpm. Batch tests were conducted using 10 L of freshly collected PI grab samples from a municipal wastewater treatment plant in Winnipeg, Canada. The PI was sampled from a concrete channel post-grit removal – Table 1. Each set of conditions was examined in triplicate, on different PI grab samples, to obtain representative results.

Table 1. Characteristics of primary influent grab samples.

Parameter	Minimum	Average	Maximum
Alkalinity (mg-$CaCO_3$/L)	270	340 ± 30	390
Conductivity (mS/cm^2)	2.0	2.4 ± 0.3	2.8

pH (-)	7.0	7.5 ± 0.2	7.9
COD (mg/L)	180	300 ± 80	490
TN (mg/L)	35	40 ± 3	47
TP (mg/L)	3.9	4.5 ± 0.3	5.0

The electrochemical cell consisted of a submerged anode and cathode, both the same material (i.e., either aluminum, iron, or magnesium) as flat sheets, in the 10 L CSTR. Iron electrodes were examined with and without aeration (i.e., 2 L/min air, or 1 liquid volume every 5 min), since oxygen can convert ferrous iron to ferric iron and thereby change the chemistry of removal. The submerged dimensions were 10 cm wide by 20 cm deep, resulting in a submerged surface area of 200 cm^2. The anode and cathode were electrically connected via copper wire and a DC power supply (Model BOP 100-2D, KEPCO Inc., USA). The applied current was maintained at a fixed rate, which varied from 200 mA to 3.8 A during the study. The resulting current densities were therefore 1-20 mA/cm^2. The following half-cell reactors describe the stoichiometry of metal dissolution during electrocoagulation:

At the anode with aluminum:

$$Al_{(s)} \rightarrow Al^{3+} + 3 \cdot e^{-}$$

Once aluminum has solubilized, longer-chain aluminum hydroxides can develop depending on contact time and pH:

$$Al^{3+} + H_2O \rightarrow Al(OH)^{2+} + H^+$$

$$Al(OH)^{2+} + H_2O \rightarrow Al(OH)_2^+ + H^+$$

$$Al(OH)_2^+ + H_2O \rightarrow Al(OH)_3 + H^+$$

$$Al(OH)_3 + H_2O \rightarrow Al(OH)_4^- + H^+$$

At the anode with iron:

$$Fe_{(s)} \rightarrow Fe^{2+} + 2 \cdot e^-$$

Ferrous iron generated at the anode can be oxidized to ferric iron in the presence of oxygen:

$$4 \cdot Fe^{2+} + O_2 + 4 \cdot H^+ \rightarrow 4 \cdot Fe^{3+} + 2 \cdot H_2O$$

At the anode with magnesium:

$$Mg_{(s)} \rightarrow Mg^{2+} + 2 \cdot e^-$$

At the cathode with any electrode material:

$$2 \cdot H^+ + 2 \cdot e^- \rightarrow H_{2\,(g)} \uparrow$$

The dissolved metals could remove COD, TN, and TP through many mechanisms, including but not limited to: 1) direct precipitation of ionic species such as orthophosphate (e.g., as metal-hydroxide complexes) and ammonium (e.g., magnesium ammonium phosphate); 2) entrapment of both ionic and organic species in larger flocs such as

hydroxides; and 3) micro-flocculation of colloidal particles via destabilization with metal ions (i.e., disruption of the electrical double layer).

2.3. Analytical methods and calculations

Samples were analyzed for COD, total nitrogen (TN), total phosphorus (TP; TNTplus, Hach, CA), total ammonia nitrogen (TAN), nitrite nitrogen, nitrate nitrogen, and orthophosphate (OP; Lachat QuikChem 8500, HACH, CA). The removal of organic, nitrogen, and phosphorus fractions was calculated according to Equation 1.

$$Removal = \frac{C_O - C}{C_O} \cdot 100 \quad (1)$$

Where removal (i.e., %) was calculated as the difference between initial (i.e., C_O, mg/L) and final (i.e., C, mg/L) concentrations divided by the initial concentration multiplied by 100.

Samples for total suspended solids (TSS), volatile suspended solids (VSS), and alkalinity were analyzed according to standard methods [21]. Measurements of pH and conductivity were performed using probes (accumet Excel XL50, Fisher Scientific, USA). Nitrification rates were quantified twice; once as the ammonium utilization rate (AUR) and then again as the nitrite/nitrate production rate (NPR). The only difference between AUR and NPR is that the AUR included incorporation of ammonium nitrogen into new biomass and was therefore not a true representation of autotrophic nitrogen removal. However, for these experiments the AUR served as an additional level of certainty. NPR (i.e., Equation 2) was calculated from kinetic test data (i.e., the slope of nitrite/nitrate production) and was expressed as mg-NOx-N/(g-VSS•h). NPR describes the increase of nitrite/nitrate concentration in a unit of time with respect to the amount of biomass. Analogically, AUR (i.e., Equation 3) was calculated from t kinetic test data (i.e., the slope of ammonium removal)

and was expressed as mg-NH_4-N/(g-VSS•h). AUR describes the decrease in ammonia concentration in a unit of time with respect the amount of biomass.

$$NPR = \frac{m_{NO_X-N\ production}}{VSS_{biomass}} \quad (2)$$

$$AUR = \frac{m_{NH_4-N\ removal}}{VSS_{biomass}} \quad (3)$$

Where m was the slope of nutrient concentration versus time and $VSS_{biomass}$ was the concentration of biomass in the kinetic test.

The production of biogas from anaerobic digestions of settled solids was quantified using an AER-800 Research Respirometer. Anaerobic digestion was maintained at 35 °C using a waterbath (PolyScience®, USA). All samples that required filtration were run through medium porosity Q5 filter paper (Fisher Scientific, CA). Solids destruction and biogas yield were calculated according to Equation 4 and Equation 5, respectively.

$$Solids\ destruction = \frac{VSS_O - VSS}{VSS_O} \cdot 100 \quad (4)$$

$$Biogas\ yield = \frac{V_{biogas}}{(VSS_O - VSS) \cdot V_{reactor}} \quad (5)$$

Where solids destruction (i.e., %) was calculated as the difference between initial (i.e., VSS_O, mg/L) and final (i.e., VSS, mg/L) concentrations divided by the initial concentration multiplied by 100. Biogas yield (i.e., L-biogas/g-VSS destroyed) was calculated as the total volume of biogas produced (i.e., V_{biogas}, L) divided by the product of reactor volume (i.e., $V_{reactor}$, L) and the difference between initial (i.e., VSS_O, g/L) and final (i.e., VSS, g/L) concentrations.

3. Results and discussion

3.1. General performance

The first set of experiments performed at 600 mA with an electrolysis time of 30 min and settling time of 45 min provided insight on how aluminum, iron, and magnesium electrodes performed under similar conditions – Figure 1. Aluminum electrodes provided the best and most reliable removal of COD. Observed removal of COD with aluminum electrodes was 68±9%, while observed TN and TP removals were 10±20% and 70±20%, respectively. Aluminum electrodes also removed 28±5% of sCOD, -12±5% of TAN (i.e., negative value represents potentially hydrolysis of organic nitrogen), and 92±2% of OP. Observed COD, TN, and TP removal with iron electrodes ranged from 40±30%, 10±30%, and 90±20%, respectively. Iron electrodes also removed 30±20% of sCOD, -5±8% of TAN, and 92±4% of OP.

Overall, magnesium electrodes provided the worst treatment. At 600 mA applied for 30 min, the observed removal of COD, TN, and TP with magnesium electrodes ranged from 27±3%, 5±2%, and 18±2%, respectively. Magnesium electrodes removed 8±5% of sCOD, 2±3% of TAN, and 21±7% of OP. All treatments with electrodes enhanced the removal of COD, TN, and TP during sedimentation compared to the control, which removed 14±2% of COD, 3±4% of TN, and 6±8% of TP. The control also removed -3±5% sCOD, 2±3% TAN, and 3±5% OP (i.e., negligible removal of soluble species). In all cases COD and TP removals were the most improved in all cases, compared to the control, while the least benefit was observed with regards to TN removal.

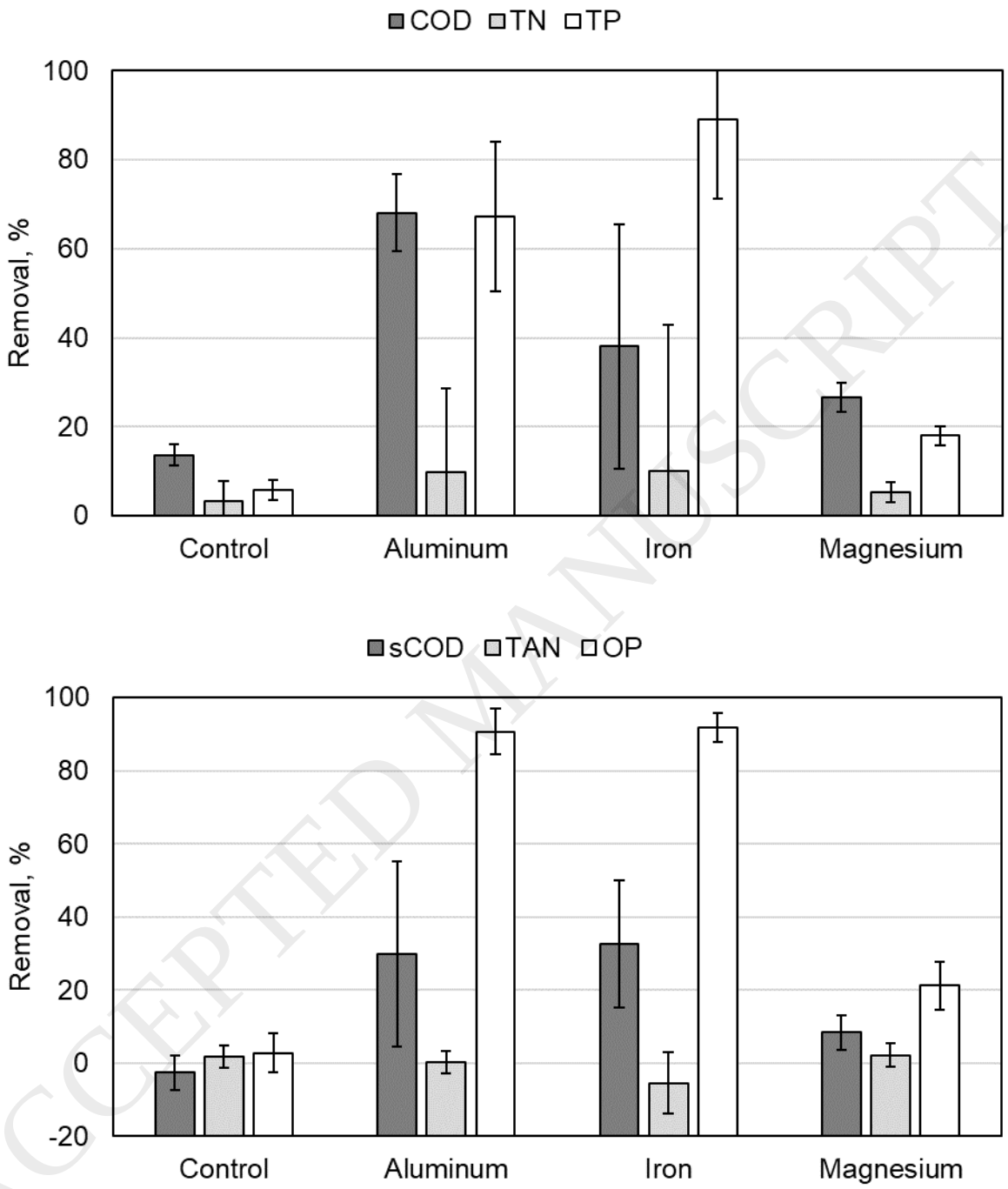

Figure 1. Top – Removal of COD, TN, and TP with aluminum, iron, and magnesium electrodes at 600 mA applied for 30 min followed by a 45 min settling period; Bottom – Removal of sCOD, TAN, and OP with aluminum, iron, and magnesium electrodes at 600

mA applied for 30 min followed by a 45 min settling period. The control included only the 45 min settling period. Error bars represent one standard deviation.

Compared to an equivalent dose of alum and ferric as metal salts (i.e., 0.6 mmol-Me/L), aluminum and iron electrodes with 600 mA applied for 30 min provided similar COD, TN, and TP removals – Figure 2. Alum salt removed 70±30% of COD, 10±20% of TN, and 70±20% of TP. Compared to aluminum electrodes, alum was only capable of removing up to an additional 3.4% of TN and 18.3% of TP. Alum salt did not remove additional COD. Similarly, ferric salt was observed to remove 50±10% of COD, 11±1% of TN, and 91±5% of TP. Compared to iron electrodes, ferric salt removed up to an additional 12% of COD, 1% of TN, and 2.2% of TP. Compared to aluminum and iron electrodes, alum salt and ferric salt did not remove additional sCOD, TAN, or OP.

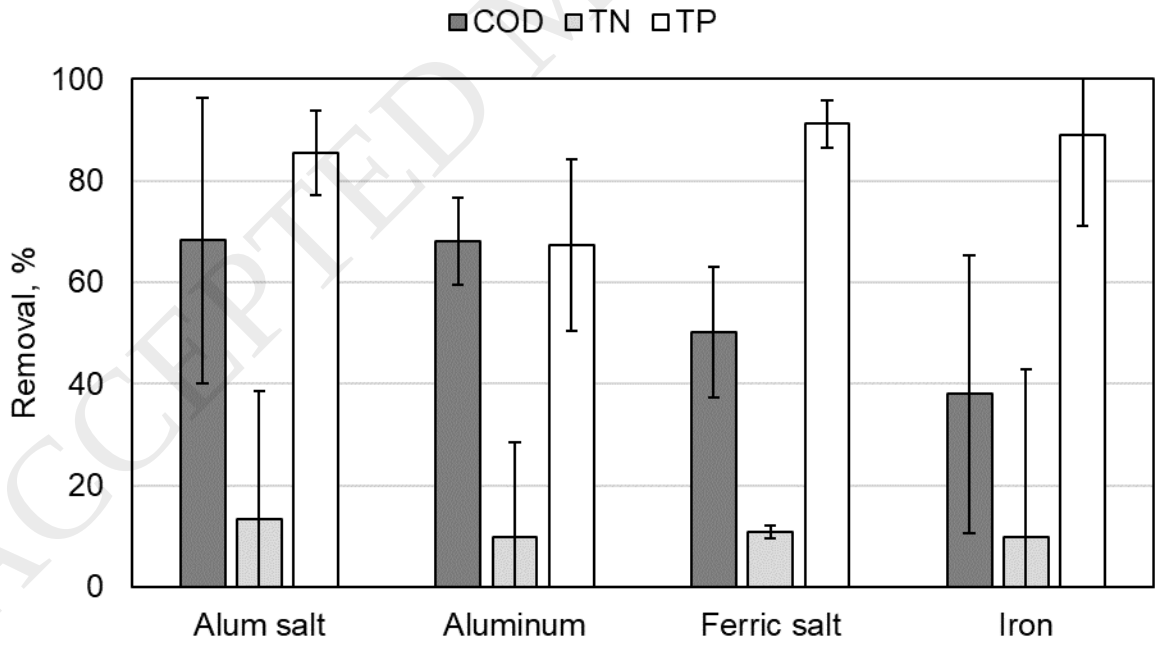

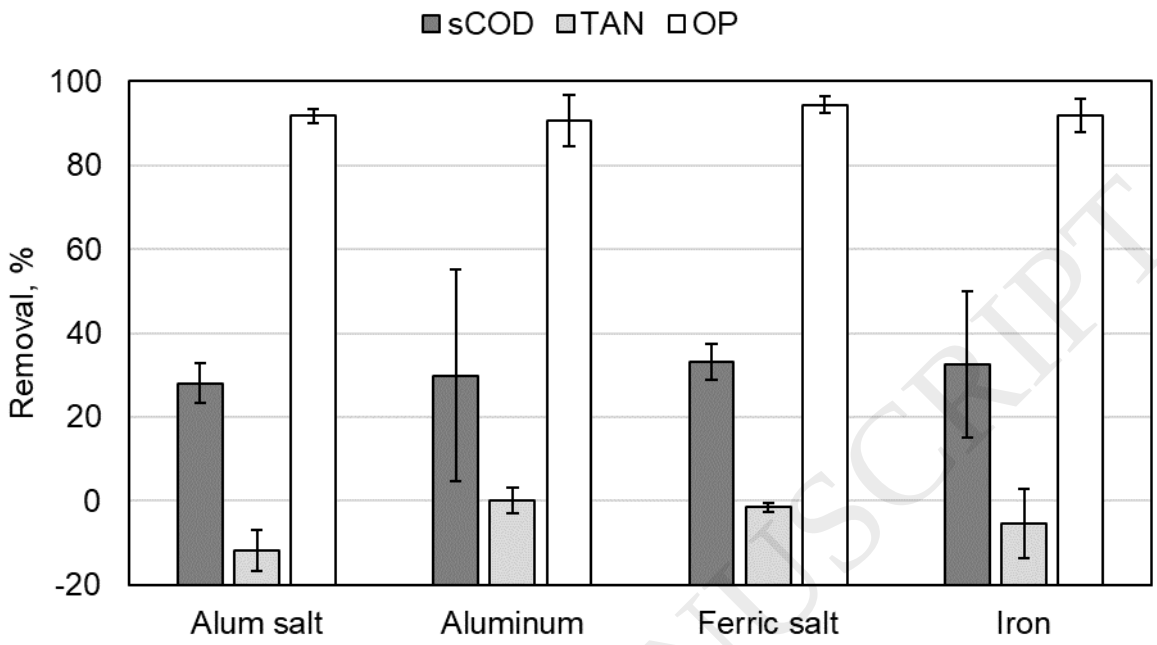

Figure 2. Top – Removal of COD, TN, and TP with aluminum and iron electrodes at 600 mA applied for 30 min followed by a 45 min settling period. Shown with COD, TN, and TP removals for an equivalent dose (0.6 mmol-Me/L) of metal salt; Bottom – Removal of sCOD, TAN, and OP with aluminum and iron electrodes at 600 mA applied for 30 min followed by a 45 min settling period. Shown with sCOD, TAN, and OP removals for an equivalent dose (0.6 mmol-Me/L) of metal salt. Error bars represent one standard deviation.

These results demonstrated that an unoptimized electrocoagulation process could achieve comparable results to metal salt addition. It is interesting to note that alum salt removed more TP than aluminum electrodes, while ferric salt removed more COD that iron electrodes. The reason for alum salt's increased TP removal performance may be pH related. The pH of the raw wastewater was 7.6±0.1, while the pH of wastewater treated with alum salt was 6.3±0.2 and the pH of wastewater treated with aluminum electrodes was 7.6±0.7. Minimum solubility of aluminum occurs at pH 6-7 [22], thus aluminum would have been

less soluble when alum salt was used. The lower solubility of aluminum with alum salt addition may explain the higher TP removal, since more aluminum would have been available for precipitation/entrapment. Similarly, the improved COD removal by ferric salt may be explained by pH. The minimum solubility of ferric iron occurs at pH 8 [23] and ferrous iron occurs at pH >11 [24]. Without aeration, the iron electrodes would have been generating ferrous iron [25], which would have been more soluble than the ferric dosed as salt. It may be that ferric removed more COD due to its lower solubility at the final pH of reaction and thereby more adsorption/entrapment of organic matter by ferric. Furthermore, the higher charge of ferric compared to ferrous may have contributed to enhanced destabilization of the electrical double layer, thereby resulting in micro-flocculation of colloidal particles and their removal. Although ferric has a higher charge than ferrous, there would be significantly less soluble ferric iron than soluble ferrous iron at the pH of reaction and therefore enhanced particle destabilization was not likely a contributing factor to the higher removal of COD by ferric.

It should be noted that there was a significant difference in pH and alkalinity between aluminum and iron electrodes and their metal salt counterparts. During electrocoagulation, the pH and alkalinity slightly increased during treatment. However, metal salt addition resulted in a significant decrease in both pH and alkalinity. The initial and final pH for alum salt treatment ranged from 7.60-7.64 and 6.67-6.73, respectively. Similarly, the initial and final pH for ferric salt treatment ranged from 7.61-7.70 and 7.04-7.18, respectively. Regarding alkalinity, the initial and final values with alum salt ranged from 340-350 mg-$CaCO_3$/L and 160-190 mg-$CaCO_3$/L, respectively. The initial and final alkalinity for ferric

salt ranged from 350-355 mg-$CaCO_3$/L and 270-280 mg-$CaCO_3$/L, respectively. In general, the alum salt had the greatest impact on pH and alkalinity. Overall, the electrocoagulation process would have a positive impact on downstream biological treatment, especially aerobic, autotrophic nitrogen removal which stoichiometrically requires 7.14 g-$CaCO_3$/g-N removed [26].

The performance of iron electrodes was also examined in the absence and presence of aeration – Figure 3. In general, aeration had no significant impact on the removal of TN or TP with iron electrodes. However, COD removal did increase significantly. In the presence of 2 L/min air (i.e., 1 liquid volume every 5 min), iron electrodes removed 60±30% of COD, 12±3% TN, and 93±5% of TP. Thus, the speciation of iron generated during electrocoagulation did have a significant impact on COD removal during sedimentation. In fact, COD removal with iron electrodes in the presence of aeration was like COD removal with ferric salt, suggesting that ferric was better at removing COD than ferrous. As previously mentioned, this was likely because ferric was less soluble than ferrous at the pH of solution, resulting in more adsorption/entrapment of organic matter.

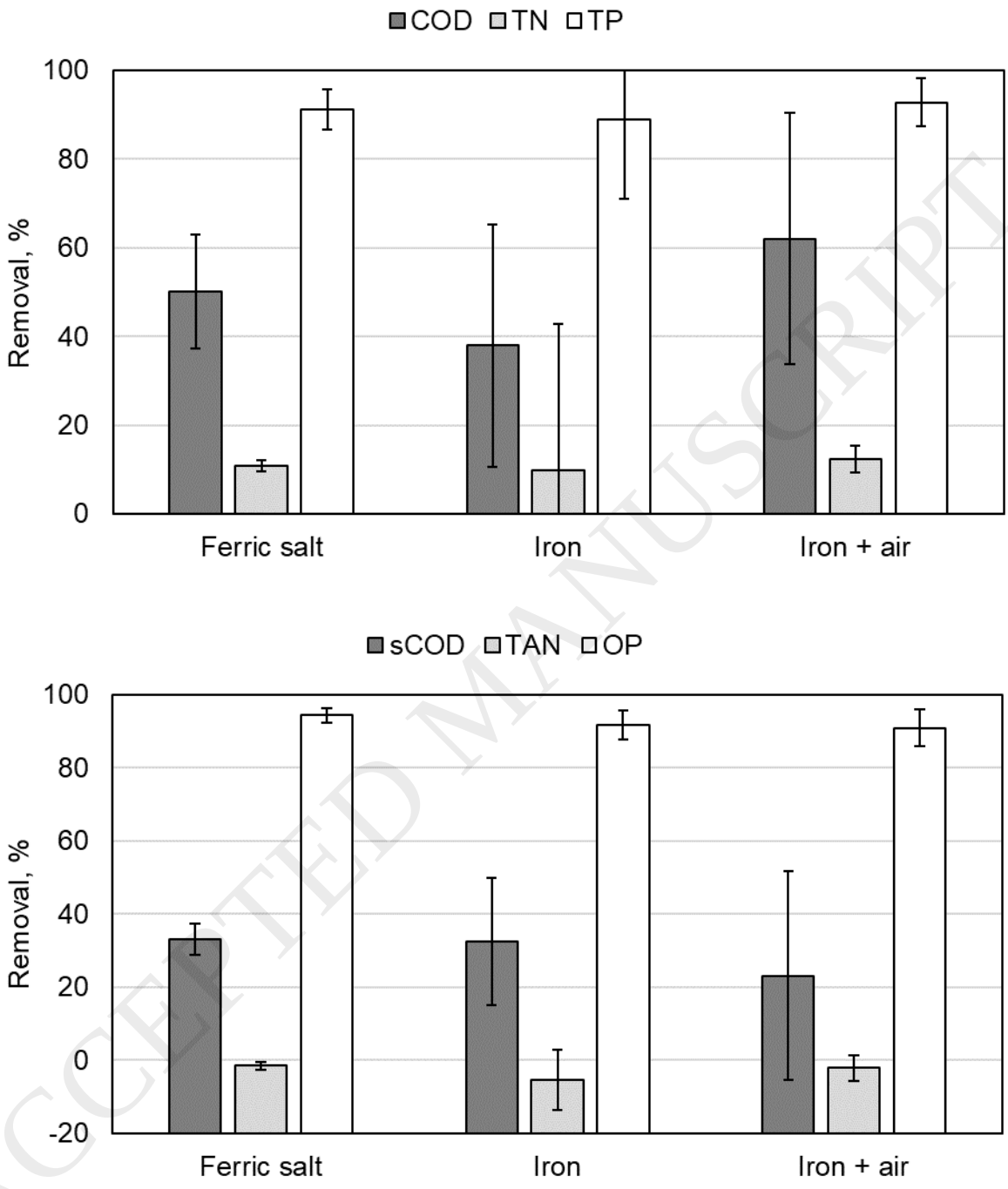

Figure 3. Top – Removal of COD, TN, and TP with iron electrodes in the absence or presence of aeration at 600 mA applied for 30 min followed by a 45 min settling period. Shown with COD, TN, and TP removals for an equivalent dose (0.6 mmol-Me/L) of metal salt; Bottom

– Removal of sCOD, TAN, and OP with iron electrodes in the absence or presence of aeration at 600 mA applied for 30 min followed by a 45 min settling period. Shown with sCOD, TAN, and OP removals for an equivalent dose (0.6 mmol-Me/L) of metal salt. Error bars represent a single standard deviation.

3.2. Orthophosphate removal rates

Aluminum, iron, and magnesium electrodes were studied under various current intensities and electrolysis times for OP removal – Figure 4. The removal rate of OP per electron moles dosed (i.e., product of current intensity and electrolysis time divided by Faraday's constant) were similar for aluminum and iron electrodes. In fact, the combined dataset for OP residual as a function of electron dose for aluminum and iron electrodes, with and without aeration, had a strong correlation (i.e., $R^2 = 0.7972$). The overall removal rate of OP for aluminum and iron electrodes, with and without aeration, was observed to be 6.8 mg-P/mmol-e. It was interesting to note that below 0.1 mmol-e/L, there appeared to be insignificant OP removal with aluminum and iron electrodes. This may be due to several reasons, including aluminum and iron still being within solubility limits or the fact that aluminum and iron hydroxides had to develop before OP was removed. Unlike the other electrode materials, magnesium electrodes had a much slower rate of OP removal per electron moles dosed. The observed OP removal rate was only 0.9 mg-P/mmol-e (i.e., $R^2 = 0.8255$). This was almost 8 times slower than the OP removal rates observed for aluminum and iron electrodes.

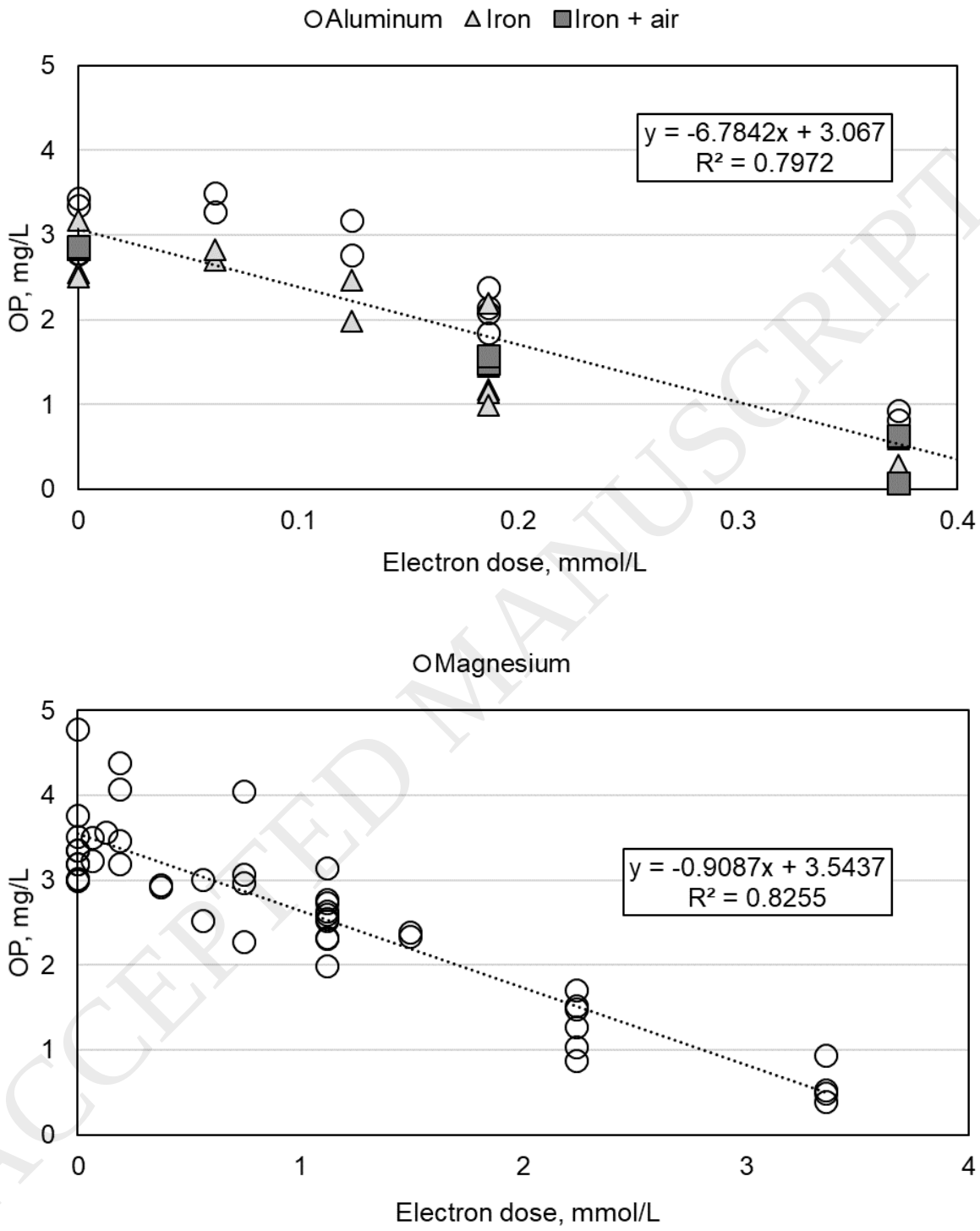

Figure 4. Top – OP residual as a function of electron dose for aluminum and iron electrodes; Bottom – OP residual as a function of electron dose for magnesium electrodes.

Assuming $Al^{3+}_{(aq)}$ and $Fe^{2+}_{(aq)}$ were produced at the anode with aluminum and iron electrodes (i.e., oxygen oxidizes $Fe^{2+}_{(aq)}$ to $Fe^{3+}_{(aq)}$ after it is generated at the anode), respectively, the theoretical molar ratio of metal dosed to OP removed for aluminum would be 1.3 and for iron would be 4.1. Assuming $Mg^{2+}_{(aq)}$ was produced at the anode, the molar ratio of metal dosed to OP removed was approximately 13.5. These results indicated that OP removal with magnesium electrodes was not dose dependent, since the molar ratios of magnesium to OP for magnesium ammonium phosphate (i.e., struvite) and magnesium phosphate are 1 and 1.5, respectively [27]. These are much lower than the observed molar ratio of 13.5.

The lower OP removal rates observed for magnesium electrodes may be explained by pH dependent solubility relationships – Figure 5. For instance, the pH never increased more than 1 unit before the OP was completely removed with aluminum or iron electrodes. In fact, the pH never rose above 8 with aluminum or iron electrodes to completely remove OP. Minimum solubility of aluminum occurs at pH 6-7 [22], while minimum solubility of ferric iron occurs at pH 8 [23] and ferrous iron occurs at pH >11 [24]. Thus, aluminum electrodes and iron electrodes, with aeration (i.e., ferric production), would have been producing metal species within the range of their minimum solubility, since pH varied from 7 to 8 for complete OP removal. Precipitation/entrapment, both in bulk solution or localized precipitation at the surface of electrodes, was likely the major removal mechanism in these cases. Due to the short run time of the experiments, phosphorus precipitation on the surface of the electrodes was not visually observed. Experiments with longer run times and probably continuous flow would be required to asses the details of precipitation on electrodes. However, iron electrodes

without aeration would have been producing ferrous iron, which would not have been near minimum solubility. Regardless, the removal of OP was not impacted by the lower solubility of the reactive metal species (i.e., ferrous iron).

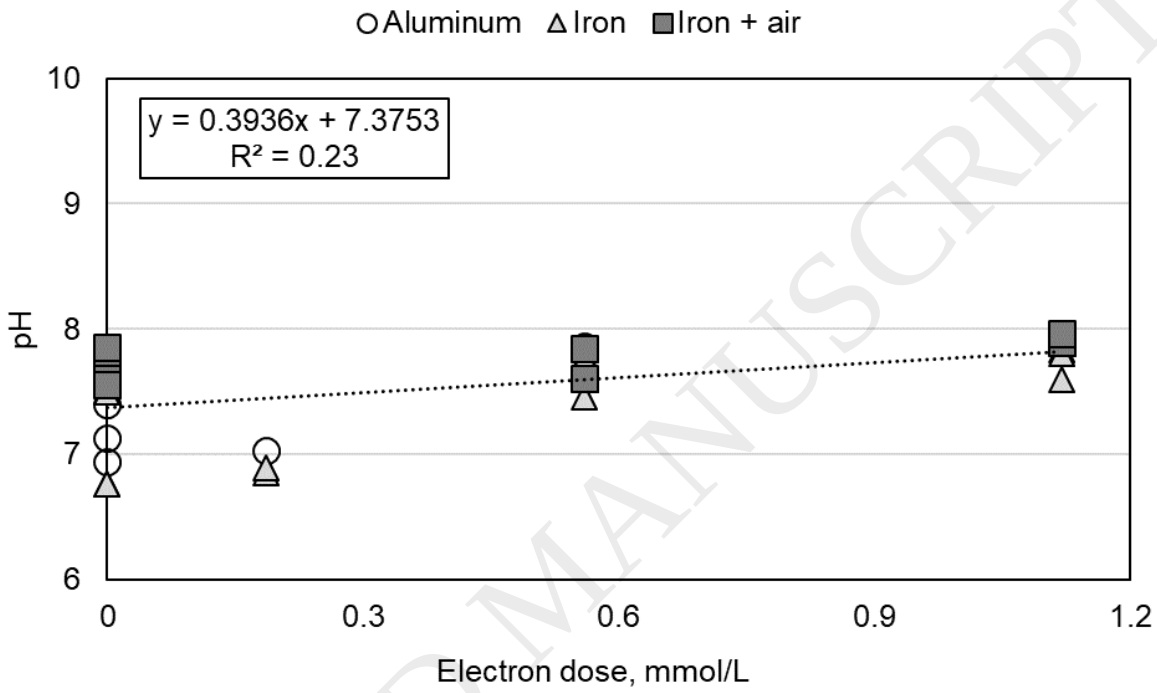

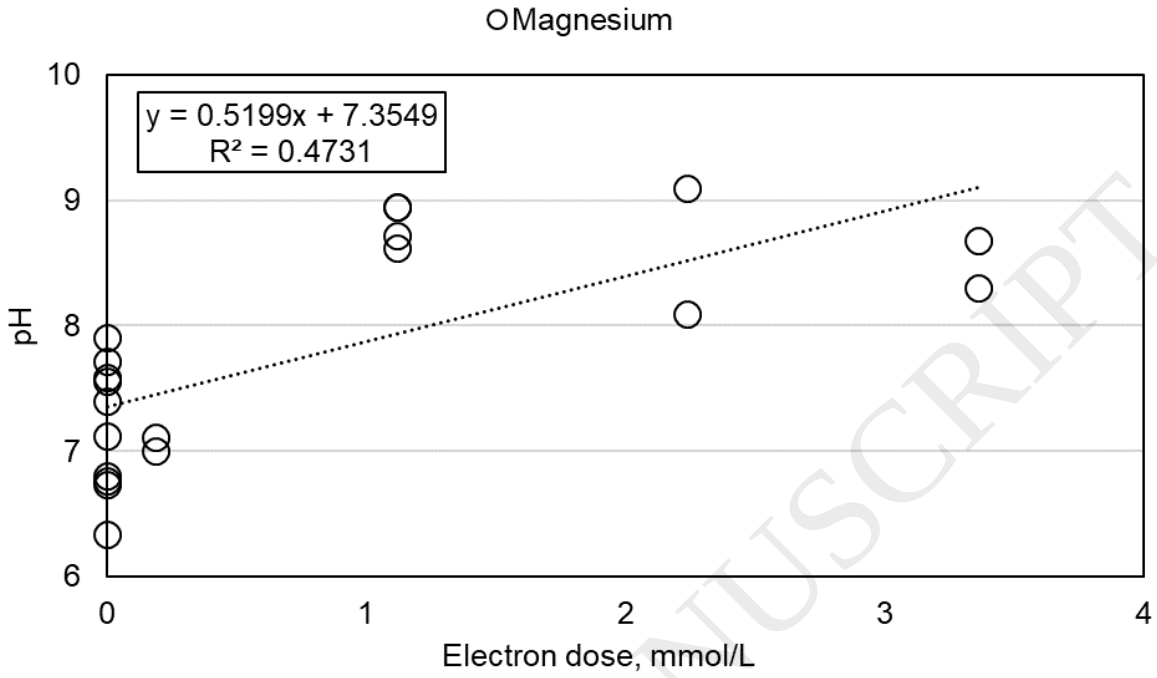

Figure 5. Top – pH as a function of electron dose for aluminum and iron electrodes; Bottom – pH as a function of electron dose for magnesium electrodes.

On the other hand, complete OP removal with magnesium electrodes required a final pH of 8.5-9. This may be explained by the fact that minimum solubility of magnesium occurs as pH rises above 8 [23]. Therefore, significant magnesium precipitation reactions may not have occurred until the pH rose above 8.5. It should also be noted that COD and TN removal with magnesium electrodes also increased with pH. The maximum observed COD and TN removals with magnesium electrodes occurred at pH greater than 8.5 and were 49% and 21%, respectively (i.e., at an electron dose of 2.3 mmol-e/L). The initial results for magnesium, performed at 600 mA for 30 min (i.e., electron dose of 1.11 mmol-e/L) were 27±3% COD removal and 5±2% TN removal.

It is interesting to note that the rate of increase in pH was similar between aluminum, iron, and magnesium electrodes. The grouped dataset had a rate of increase in pH of 0.39 pH units/mmol-e (i.e., $R^2 = 0.23$). The rate of pH increase with magnesium electrodes was 0.52 pH units/mmol-e (i.e., $R^2 = 0.4731$), respectively. Similarly, the rate of increase in alkalinity was comparable between aluminum, iron, and magnesium electrodes. The observed rate of increase in alkalinity with aluminum, iron, and magnesium electrodes was 11.4 mg-$CaCO_3$/mmol-e (i.e., $R^2 = 0.0592$), 21.7 mg-$CaCO_3$/mmol-e (i.e., $R^2 = 0.1816$), and 39.6 mg-$CaCO_3$/mmol-e (i.e., $R^2 = 0.5612$), respectively. The similarity in pH and alkalinity trends between all electrodes was likely a result of a single reaction dominating the cathode (i.e., Equation 9).

3.3. Nitrification kinetics and biogas production

Supernatant after treatment with aluminum, iron, and magnesium electrodes at 200 mA applied for 15 min followed by 45 min of settling was examined for nitrification rates at 20 °C and saturated dissolved oxygen – Figure 7. AUR was 1.20±0.05 mg-N/(g-VSS•h) for the control, 1.4±0.1 mg-N/(g-VSS•h) with aluminum electrodes, 1.2±0.1 mg-N/(g-VSS•h) with iron electrodes, and 1.29±0.06 mg-N/(g-VSS•h) with magnesium electrodes. NPR was 1.2±0.2 mg-N/(g-VSS•h) for the control, 1.5±0.1 mg-N/(g-VSS•h) with aluminum electrodes, 1.3±0.1 mg-N/(g-VSS•h) with iron electrodes, and 1.2±0.1 mg-N/(g-VSS•h) with magnesium electrodes. There was no significant difference in nitrification between the control and iron electrodes (i.e., P-value of 0.6782) or between the control and magnesium electrodes (i.e., P-value of 0.6349). However, there was a significant difference in nitrification rates between the control and aluminum electrodes (i.e., P-value of 0.0016).

Therefore, aluminum electrodes had a significant positive on nitrification rates, most likely due to the higher COD removal by aluminum electrodes (i.e., 5 times higher than the control, 1.8 times higher than iron electrodes, 2.6 times higher than magnesium electrodes). Thus, nitrifiers may have had less competition for oxygen while removing ammonia from the wastewater treated with aluminum electrodes [13]. Long-term studies would be required to further assess the impact of electrocoagulation during primary treatment on microbial community changes in subsequent biological processes, such as activated sludge or lagoons.

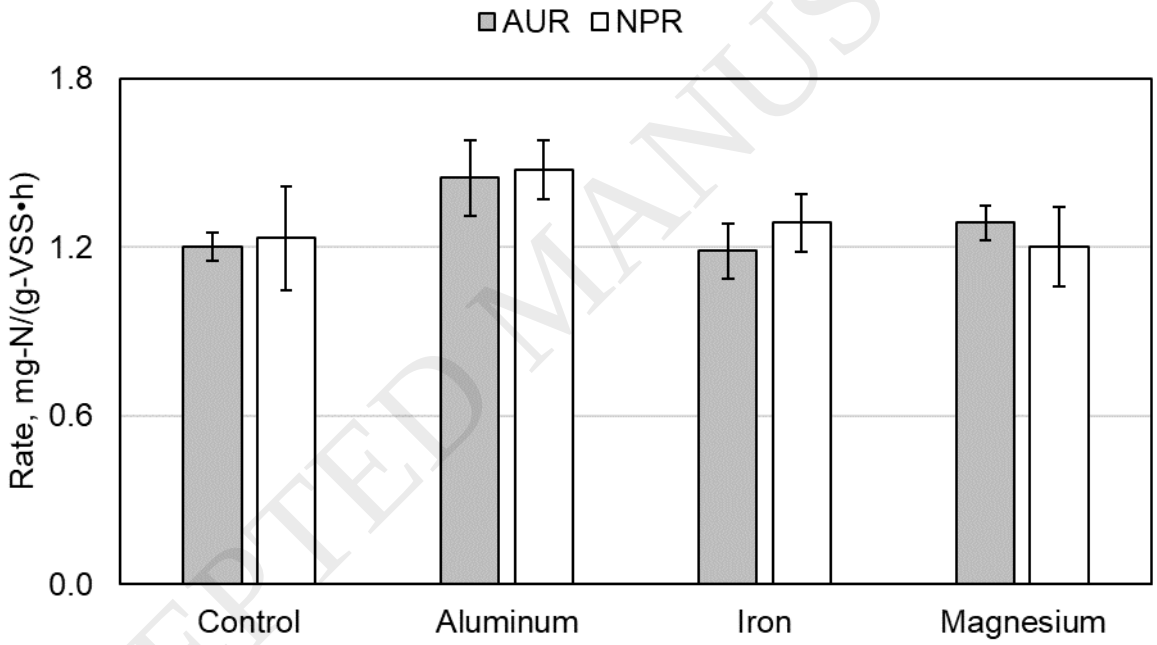

Figure 7. AUR and NPR at 20 °C and saturated dissolved oxygen on supernatant from primary influent treated by electrocoagulation with sacrificial aluminum, iron, or magnesium anodes after 45 min settling.

Settled solids from the same treatments (i.e., 200 mA applied for 15 min followed by 45 min settling) were examined for solids destruction and biogas yields under anaerobic conditions at 35 °C – Figure 8. The solids destruction ranged from 7-15% in all cases. The

average volatile solids destruction for the control was observed to be 7±6%, while the average solids destruction for treatment with aluminum electrodes was 10±15%, with iron electrodes was 15±5%, and with magnesium electrodes was 10±10%. Although solids destruction was higher in the samples with electrocoagulation, the difference in solids destruction between the control and any of the treatments was not statistically different (i.e., P-value = 0.3083 for aluminum, 0.0663 for iron, and 0.4613 for magnesium). Biogas yields ranged from 0.12-0.44 L/g-VSS destroyed in all cases. The average biogas yield for the control was observed to be 0.4±0.4 L/g-VSS destroyed while the average biogas yield for treatment with aluminum electrodes was 0.3± 0.4 L/g-VSS destroyed, with iron electrodes was 0.12±0.05 L/g-VSS destroyed, and with magnesium electrodes was 0.2±0.2 L/g-VSS destroyed. The difference in biogas yield between the control and any of the treatments were not determined to be statistically different (i.e., P-value = 0.3849 for aluminum, 0.0950 for iron, and 0.9295 for magnesium).

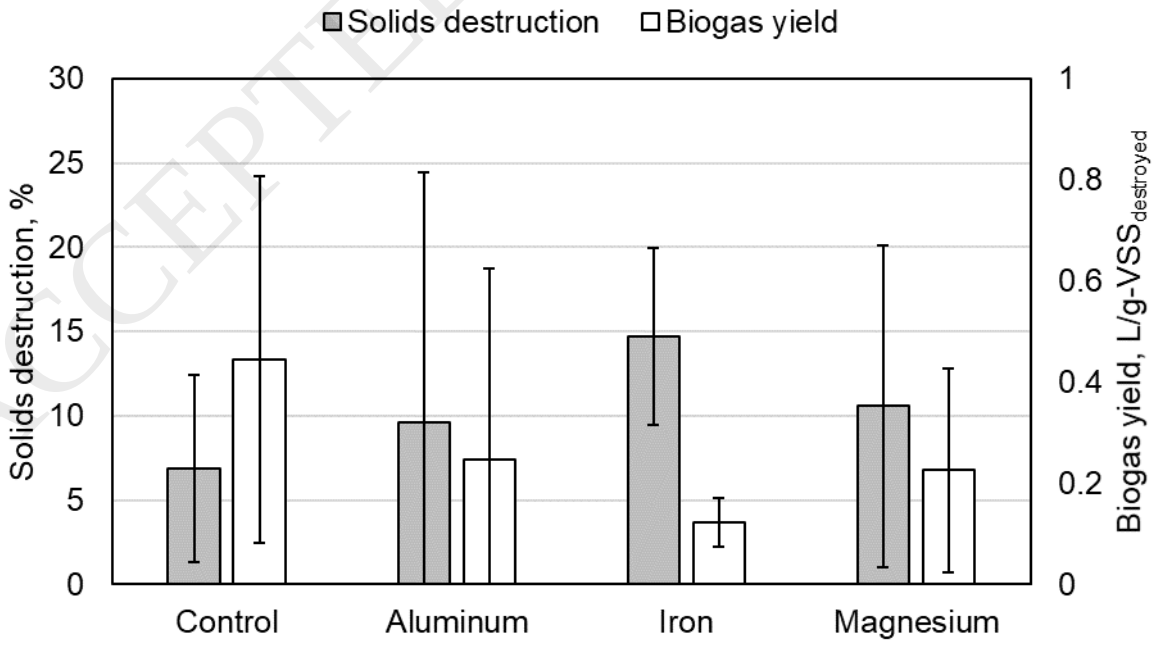

Figure 8. Solids destruction and biogas yields at 35 °C on settled solids from primary influent treated by electrocoagulation with sacrificial aluminum, iron, or magnesium anodes after 45 min settling.

4. Conclusions

Electrocoagulation was used to enhance the removal of COD, TN, and TP during sedimentation. Electrocoagulation with sacrificial aluminum or iron anodes provided similar treatment to equivalent metal doses of alum and ferric salts. The maximum observed OP removal rates with aluminum and iron electrodes were 6.8 mg-P/mmol-e. Magnesium electrodes required higher electron doses (i.e., ~2.7 mmol-e/L) to remove equivalent amounts of OP when aluminum or iron electrodes were used (i.e., 0.3 mmol-e/L). As well, the maximum observed OP removal rate with magnesium electrodes was only 0.9 mg-P/mmol-e, which was more than 7 times lower than the rates observed with aluminum or iron electrodes. The estimated molar ratio of metal dosed to OP removed was determined to be approximately 1.3 for aluminum electrodes, 4.1 for iron electrodes, and 13.5 for magnesium electrodes. While the removal of OP by aluminum and iron electrodes occurred within the expected stoichiometric range, the removal of OP by magnesium electrodes required significantly higher magnesium. This was probably due to the minimum solubility of magnesium increasing as pH rises to 10.5. Thus, cathodic reactions, which raise the pH, were likely the rate limiting step for magnesium electrodes. Thus, future studies may examine pH adjustment with magnesium electrodes in order to facilitate more economic treatment. Overall, all electrode materials enhanced the performance of primary sedimentation. Furthermore, electrocoagulation with aluminum electrodes significantly improved

nitrification rates. If electrocoagulation with iron and magnesium electrodes was optimized for COD removal, it is possible that they would have had a positive impact on nitrification as well.

References

[1] J. Oleszkiewicz, D. Kruk, T. Devlin, Options for improved nutrient removal and recovery from municipal wastewater in the Canadian context, 2015.

[2] K. Daley, H. Castleden, R. Jamieson, C. Furgal, L. Ell, Water systems, sanitation, and public health risks in remote communities: Inuit resident perspectives from the Canadian Arctic, Soc. Sci. Med. 135 (2015) 124–132. doi:10.1016/j.socscimed.2015.04.017.

[3] M. Anda, K. Mathew, G. Ho, Evapotranspiration for domestic wastewater reuse in remote indigenous communities of Australia, Water Sci. Technol. 44 (2001) 1–10.

[4] N. Ashbolt, Microbial contamination of drinking water and disease outcomes in developing regions, Toxicology. 198 (2004) 229–238.

[5] A. Prüss, L. Fewtrell, J. Bartam, Estimating the burden of diseases from water, sanitation, and hygeine at a global level, Envrionmental Heal. Perspect. 110 (2002) 537–542.

[6] Environment Canada, The state of municipal wastewater effluents in Canada, 2001.

[7] G.E. Üstün, Occurrence and removal of metals in urban wastewater treatment plants, J. Hazard. Mater. 172 (2009) 833–838. doi:10.1016/j.jhazmat.2009.07.073.

[8] M.I. Badawy, R.A. Wahaab, A.S. El-Kalliny, Fenton-biological treatment processes for the removal of some pharmaceuticals from industrial wastewater, J. Hazard. Mater. 167 (2009) 567–574. doi:10.1016/j.jhazmat.2009.01.023.

[9] J.H. Chang, T.J. Yang, C.H. Tung, Performance of nano- and nonnano-catalytic electrodes for decontaminating municipal wastewater, J. Hazard. Mater. 163 (2009)

152–157. doi:10.1016/j.jhazmat.2008.06.072.

[10] E.S. Elmolla, M. Chaudhuri, Combined photo-Fenton-SBR process for antibiotic wastewater treatment, J. Hazard. Mater. 192 (2011) 1418–1426. doi:10.1016/j.jhazmat.2011.06.057.

[11] R. Gupta, V.K. Garg, Stabilization of primary sewage sludge during vermicomposting, J. Hazard. Mater. 153 (2008) 1023–1030. doi:10.1016/j.jhazmat.2007.09.055.

[12] S. Chen, N. Li, B. Dong, W. Zhao, L. Dai, X. Dai, New insights into the enhanced performance of high solid anaerobic digestion with dewatered sludge by thermal hydrolysis: Organic matter degradation and methanogenic pathways, J. Hazard. Mater. 342 (2018) 1–9. doi:10.1016/j.jhazmat.2017.08.012.

[13] J.M. Gálvez, M.A. Gómez, E. Hontoria, J. González-López, Influence of hydraulic loading and air flowrate on urban wastewater nitrogen removal with a submerged fixed-film reactor, J. Hazard. Mater. 101 (2003) 219–229. doi:10.1016/S0304-3894(03)00173-0.

[14] H. Carrère, C. Dumas, A. Battimelli, D.J. Batstone, J.P. Delgenès, J.P. Steyer, I. Ferrer, Pretreatment methods to improve sludge anaerobic degradability: A review, J. Hazard. Mater. 183 (2010) 1–15. doi:10.1016/j.jhazmat.2010.06.129.

[15] M. Hutnan, M. Drtil, A. Kalina, Anaerobic stabilisation of sludge produced during municipal wastewater treatment by electrocoagulation, J. Hazard. Mater. 131 (2006) 163–169. doi:10.1016/j.jhazmat.2005.09.032.

[16] M.Y. Mollah, R. Schennach, J.R. Parga, D.L. Cocke, Electrocoagulation (EC)--science and applications., J. Hazard. Mater. 84 (2001) 29–41. doi:10.1016/S0304-

3894(01)00176-5.

[17] M.F. Pouet, A. Grasmick, Urban wastewater treatment by electrocoagulation and flotation, Water Sci. Technol. 31 (1995) 275–283.

[18] T.R. Devlin, A. Di Biase, V. Wei, M. Elektorowicz, J.A. Oleszkiewicz, Removal of soluble phosphorus from surface water using iron (Fe-Fe) and aluminum (Al-Al) Electrodes, Environ. Sci. Technol. 51 (2017). doi:10.1021/acs.est.7b02353.

[19] B. Zhang, B. Sun, M. Ji, H. Liu, Population dynamic succession and quantification of ammonia-oxidizing bacteria in a membrane bioreactor treating municipal wastewater, J. Hazard. Mater. 165 (2009) 796–803. doi:10.1016/j.jhazmat.2008.10.116.

[20] D.J. Kruk, M. Elektorowicz, J.A. Oleszkiewicz, Struvite precipitation and phosphorus removal using magnesium sacrificial anode, Chemosphere. 101 (2014) 28–33. doi:10.1016/j.chemosphere.2013.12.036.

[21] APHA, AWWA, WEF, Standard methods for the examination of water & wastewater, 22nd ed., 2012.

[22] K. Bensadok, S. Benammar, F. Lapicque, G. Nezzal, Electrocoagulation of cutting oil emulsions using aluminium plate electrodes, J. Hazard. Mater. 152 (2008) 423–430. doi:10.1016/j.jhazmat.2007.06.121.

[23] M.S. Oncel, A. Muhcu, E. Demirbas, M. Kobya, A comparative study of chemical precipitation and electrocoagulation for treatment of coal acid drainage wastewater, J. Environ. Chem. Eng. 1 (2013) 989–995. doi:10.1016/j.jece.2013.08.008.

[24] B. Morgan, O. Lahav, The effect of pH on the kinetics of spontaneous Fe(II) oxidation by O2 in aqueous solution - basic principles and a simple heuristic description,

Chemosphere. 68 (2007) 2080–2084. doi:10.1016/j.chemosphere.2007.02.015.

[25] I. Mishima, J. Nakajima, Application of iron electrolysis to full-scale activated sludge process for phosphorus removal, J. Water Environ. Technol. 9 (2011) 359–369.

[26] B. Li, S. Irvin, The comparison of alkalinity and ORP as indicators for nitrification and denitrification in a sequencing batch reactor (SBR), Biochem. Eng. J. 34 (2007) 248–255. doi:10.1016/j.bej.2006.12.020.

[27] D.C. Pedemonte, J.M. Garrido, Struvite crystallization versus amorphous magnesium and calcium phosphate precipitation during the treatment of a saline industrial wastewater, Water Sci. Technol. 64 (2011) 2460–2467.